

# Environmental Science Processes & Impacts

Accepted Manuscript



This is an *Accepted Manuscript*, which has been through the Royal Society of Chemistry peer review process and has been accepted for publication.

*Accepted Manuscripts* are published online shortly after acceptance, before technical editing, formatting and proof reading. Using this free service, authors can make their results available to the community, in citable form, before we publish the edited article. We will replace this *Accepted Manuscript* with the edited and formatted *Advance Article* as soon as it is available.

You can find more information about *Accepted Manuscripts* in the [Information for Authors](#).

Please note that technical editing may introduce minor changes to the text and/or graphics, which may alter content. The journal's standard [Terms & Conditions](#) and the [Ethical guidelines](#) still apply. In no event shall the Royal Society of Chemistry be held responsible for any errors or omissions in this *Accepted Manuscript* or any consequences arising from the use of any information it contains.



[rsc.li/process-impacts](http://rsc.li/process-impacts)

# 1 **Investigating the composition of dissolved organic matter in natural** 2 **water in rare earth mine using EEM-PARAFAC analysis**

3 YANG Hongxia\*, GAO Jinxu, LIU Wei, TAN Keyan  
4 (National Research Center for Geoanalysis, Beijing 100037)  
5

## 6 **Abstract**

7 In this study, we have characterized three fluorescent components of dissolved organic  
8 matter(DOM) in the surface and underground water of one rare earth elements ore district by  
9 excitation-emission matrix fluorescence spectroscopy(EEMs) coupled with parallel factor  
10 analysis(PARAFAC). Two protein-like components(C1,tyrosine and C2,tryptophan) and one  
11 humic-like component(C3) were identified by the DOM Fluor-PARAFAC model, with C3  
12 constituting more than 95% of the total DOM, while C1 and C2 occupying a tiny fraction of  
13 DOMs. The distribution of three PARAFAC-identified components was strongly influenced by the  
14 river direction, terrain and location of various water samples. The results suggested that DOMs of  
15 samples collected from downstream or central region had relatively higher fluorescence intensity  
16 than those of upstream or surrounding the center. In addition, a negative linear correlation  
17 ( $R^2=0.8465$ ) between pH (5.7~9.2) and fluorescence intensity of C3 were observed, indicating that  
18 the increase of pH might enhance the intensity of fluorescent humic-like substances. Although the  
19 fluorescence intensity of C1 and C2 were independent of pH changes, strong quenching effects of  
20 different heavy metals were presented for C1, and evident positive correlations between C2 and  
21 concentrations of rare earth metals(La, Ce, Tb, Dy, Tm, etc) were observed, which showed that  
22 tyrosine-like(C1) and tryptophan-like(C2) substances were assumably responsible for metal binding  
23 and adsorption in waters, respectively. Based on EEM-PARAFAC modeling, all the fluorescence  
24 EEMs of samples could be decomposed into a three-component model, and its potential  
25 applications in water quality monitoring and metal-binding indicator were likely to be developed  
26 in the fluorescence analysis of natural water.

27 **Keywords:** DOM; EEM-PARAFAC; natural water; rare earth mine.  
28  
29  
30

## 31 **Introduction**

32 Dissolved organic matter(DOM) plays an important role in geochemical processes of surface  
33 waters, rivers, oceans, etc. It can combine with metal ions to reduce its bioavailability and  
34 biotoxicity to aquatic systems<sup>[1,2]</sup>, meanwhile improving its solubility and ability of transference  
35 and translation by binding with organic or inorganic infectants<sup>[3]</sup>. Currently, dissolved organic  
36 matter (DOM) has attracted much attention in biogeochemical research fields due to its  
37 importance and the inherent complexity of its chemical composition, chemical structure and  
38 multiple sources<sup>[4,5,6]</sup>. The natural DOM includes a myriad of organic matters, such as humic  
39 substances and other biological compounds (e.g., carbohydrates, amino acids and fatty acids)<sup>[7,8]</sup>.  
40 The important component of DOM is humic substances including fulvic acids(FA) and humic  
41 acids(HA)<sup>[9,10]</sup>. Broadly speaking, HA and FA may be classified as special DOM in natural  
42 water<sup>[11]</sup>. Grasso and coworkers<sup>[12]</sup> postulated that HA and FA make up 25-50% of the total DOM

43 in natural water, and the remaining DOM has a composition of proteins, polysaccharides and  
44 hydrophilic organic acids. The origin, transportation and transformation of DOM may have a  
45 direct influence on the recycle and storage ability of carbon in watery environment<sup>[13]</sup>. So far, the  
46 control factors that influence the spatial/temporal distribution are based on qualitative discussions,  
47 thus making it very hard to distinguish the comparative impact degree of different controlling  
48 factors. Therefore, exploring the different components in DOM of surface and underground water  
49 in Jiangxi Mining Area, in the mean time quantitatively analyze DOM of different sources may  
50 plays a pivotal role in augmenting our understanding of DOM.

51 Excitation-emission matrix (EEM) has been widely applied in analyzing the fluorescent  
52 properties of DOM in natural watery<sup>[14,15,16]</sup>. The position of fluorescent peak may qualitatively  
53 designate the type and property of the fluorescent matter, and its fluorescent intensity may  
54 quantitatively indicate its relative concentration<sup>[17]</sup>. However, the accurate identification of a  
55 fluorescent peak in EEM is usually hampered by the overlap and interference of multiple  
56 fluorescent compositions in DOM<sup>[18,19]</sup>. Besides, this method only determines quite a few peaks in  
57 an EEM graph, causing a great quantity of data in experiment unanalyzed when it comes to large  
58 sums of samples<sup>[20]</sup>. In recent years, Stedmon and coworkers<sup>[21]</sup> have firstly used the  
59 parallel factor analysis (PARAFAC) to decipher the EEMs of a DOM fluorescent graph and  
60 identified the fluorescent fractions and the corresponding concentrations. The combination of  
61 PARAFAC and three-dimensional fluorescent spectrum is also applied in qualitative and  
62 quantitative analysis of the multicomponent mixture<sup>[22,23]</sup>. Since then, PARAFAC has been widely  
63 applied in identifying the EEM of soil-extract organic matter<sup>[24]</sup>, continental DOM<sup>[25]</sup>, polluted  
64 watery DOM<sup>[26]</sup>, sediment pore-water DOM<sup>[27]</sup> and ocean water DOM<sup>[28]</sup>.

65 By PARAFAC modeling, the composition, sources and fate of DOM has been a concern for  
66 analysis of samples collected from aquatic environments. Yao<sup>[29]</sup> determined two humic-like  
67 substances and three protein-like components of waterborne DOM from Lake Taihu and its  
68 tributaries using PARAFAC model. Yamashita<sup>[30]</sup> evaluated the spatial distribution of DOM along  
69 the coastal zone of the Florida Keys, and determined the regional autochthonous and  
70 allochthonous DOM sources. Meng<sup>[31]</sup> investigated the Zhujiang River by analyzing water  
71 samples in an upstream, urbanized area and downstream of the rivers, revealing the presence of  
72 tyrosine-like, tryptophan-like proteins, humic components, and tracking the origins of DOM in  
73 rivers. In addition, the PARAFAC modeling stimulated a broad interest in the study of close  
74 connections between DOM and its surroundings. For example, through characterizing  
75 PARAFAC-derived DOM components from all titrated samples, the binding of heavy metal with  
76 DOM in lake sediments was assessed for further understanding the migration and toxicity of  
77 heavy metals<sup>[32]</sup>. Binding of DOM with heavy metals, especially the rare earth elements, have  
78 been widely studied in literatures. Yamamoto<sup>[33]</sup>, Jennifer<sup>[34]</sup> and Marsac<sup>[35]</sup> reported the  
79 complexation of rare earth elements (REEs) with humic acid at different REE loading levels in  
80 aqueous environments. Pourret<sup>[36]</sup> and Sonke<sup>[37]</sup> used humic ion-binding model V to analyse  
81 REE-humic substances complexation. These previous studies have greatly enhanced our  
82 understanding of the formation of REE-humic complexes from the experimental and modeling  
83 evidences, but there are still many questions that remain unanswered. A particularly significant  
84 one is the determination of dominant components in DOM exhibiting binding behaviors and the  
85 correlation between dissolved REE concentrations and fluorescence intensities of DOM in natural  
86 waters. Although humic substances are expected to play an important role in binding REEs, it is

87 still unknown whether other components such as protein-like substances complex with REEs and  
 88 what elements are more inclined to bound into DOM in natural waters. Such information is needed  
 89 for a better understanding of the relationship between DOM and REEs studied in a natural  
 90 REE-rich area. In addition to investigate the distribution and concentration of REEs in soils in rare  
 91 earth ore district<sup>[38,39,40,41]</sup>, there are few studies on DOM and its correlation with REE along the  
 92 rivers and tributaries within this area.

93 The Jiangxi Ore District is an ideal region to study the composition of waterborne DOM  
 94 because the overexploitation of rare earth metals in the past few years is assumed to have an  
 95 indispensable impact on the components of DOM due to their strong complexing capacity<sup>[42]</sup>.  
 96 Additionally, it is originated from Yangtze River Basin with abundant sunshine and rainfall, as the  
 97 main stream Tao River runs through the whole area with approximately 55 tributaries spreading  
 98 over the ore district, which is a typical aquatic environment with balanced water input and runoff  
 99 and suitable for sample collection. The influence of rare earth metals on natural terrestrial waters  
 100 could be revealed by the relationship between the concentrations of rare earth metals and the  
 101 components of DOM of water samples from corresponding area<sup>[35]</sup>. Our research is to determine  
 102 the DOM components of natural water by PARAFAC model, and to investigate the distribution  
 103 trends, various sources for fluorescent DOM, and how the DOM components are related to pH and  
 104 absorption or complexation of different rare earth metals. The results will be valuable to illustrate  
 105 the potential of DOM to characterize surface and underground waters in Ore District.

106

## 107 **1 Experimental**

### 108 **1.1 Sample Collection**

109 All water samples in this study were collected in the Longnan Ore District, Jiangxi, China in  
 110 April 2012. These sampling sites were distributed along the main stream and its tributaries  
 111 spreading over the ore district, which were chosen for China Geological Survey project according  
 112 to the stationing rules. Samples were collected in clean glass bottles and delivered to the lab under  
 113 cooled conditions (4°C in cooling boxes) within 48 hours. The samples were then filtered through  
 114 0.45 µm Supor filter membranes (Pall, USA) within 24 hours and stored in the dark at 4°C until  
 115 analysis within two days to minimize bacterial decomposition.

116



**Fig 1 location of the sampling sites**

117

**1.2 EEM measurement**

119 The samples were diluted with Milli-Q water prior to fluorescence analysis if absorbance  
120 values were higher than 0.04 (1 cm quartz cell, 254nm) to minimize inner filter effects<sup>[43,44,45]</sup>.  
121 Fluorescence EEMs were measured on a Hitachi F-7000 fluorescence spectrophotometer with a  
122 xenon lamp, creating high-resolution fluorescence running with band width slits of 5 nm for both  
123 excitation and emission. The scanning ranges were 220–420 nm for excitation and 250–550 nm  
124 for emission. Fluorescence readings were collected at intervals of 5-nm excitation with 2-nm  
125 emission wavelengths using a scanning speed of 1200 nm•min<sup>-1</sup>.

126

**2 PARAFAC Modeling**

128 In this study, PARAFAC was applied to DOM fluorescence EEMs and component analysis  
129 using MATLAB with the DOMFluor toolbox. Excitation emission matrix scans(EEMs) for a total  
130 of 30 samples were obtained by collecting a series of emission wavelengths ranging from 250nm  
131 to 550nm and excitation wavelengths ranging from 220nm to 420nm. The data in the region  
132 influenced by first order scatter(where Rayleigh and Raman peaks dominate the signal) and the  
133 region where emission wavelength was less than excitation wavelength should be cut and replaced  
134 with missing values or zeros. To reduce the Rayleigh scatter, data measured at emission  
135 wavelength between excitation wavelength-5nm and excitation wavelength+5nm were eliminated.  
136 After removing the Rayleigh and Raman scatters, non-negativity constraint was applied to the  
137 model, and all the loadings and leverages appeared to be more logical. Then EvalModel function  
138 was used to create a series of graphs including measured, modeled and residual EEM(Fig.2).  
139 Through Split Half analysis and validation process, the data were divided into two halves of  
140 similar curves and fit models with 3 to 7 components. Except a three component model, others  
141 could not be split-half validated. Thus, a three component model was confirmed to be adequate for  
142 split-half validation and capable of characterizing DOM of surface and underground water from  
143 Jiangxi Ore District. To create surface or contour plots of each component, the Component EEM  
144 or ComponentSurf functions could be used.

145

146

147

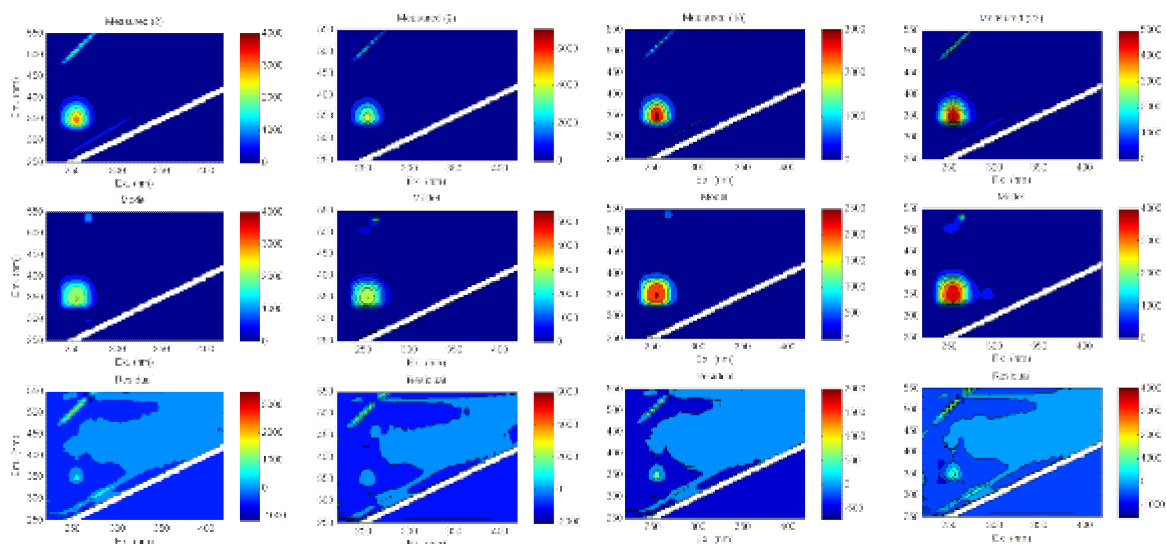


**Fig 2. Examples of measured, modeled and residual EEMs for sample collected from sites of S2(2), S8(9), S14(18), S19(23). Fluorescence is shown in Raman Units (R.U.nm<sup>-1</sup>).**

148

### 3. Results and discussion

149

#### 3.1 Fluorescence Characterization and PARAFAC analysis of EEM spectra

150

151

152

153

154

155

156

157

158

159

160

161

162

163

164

165

166

167

168

169

170

171

172

173

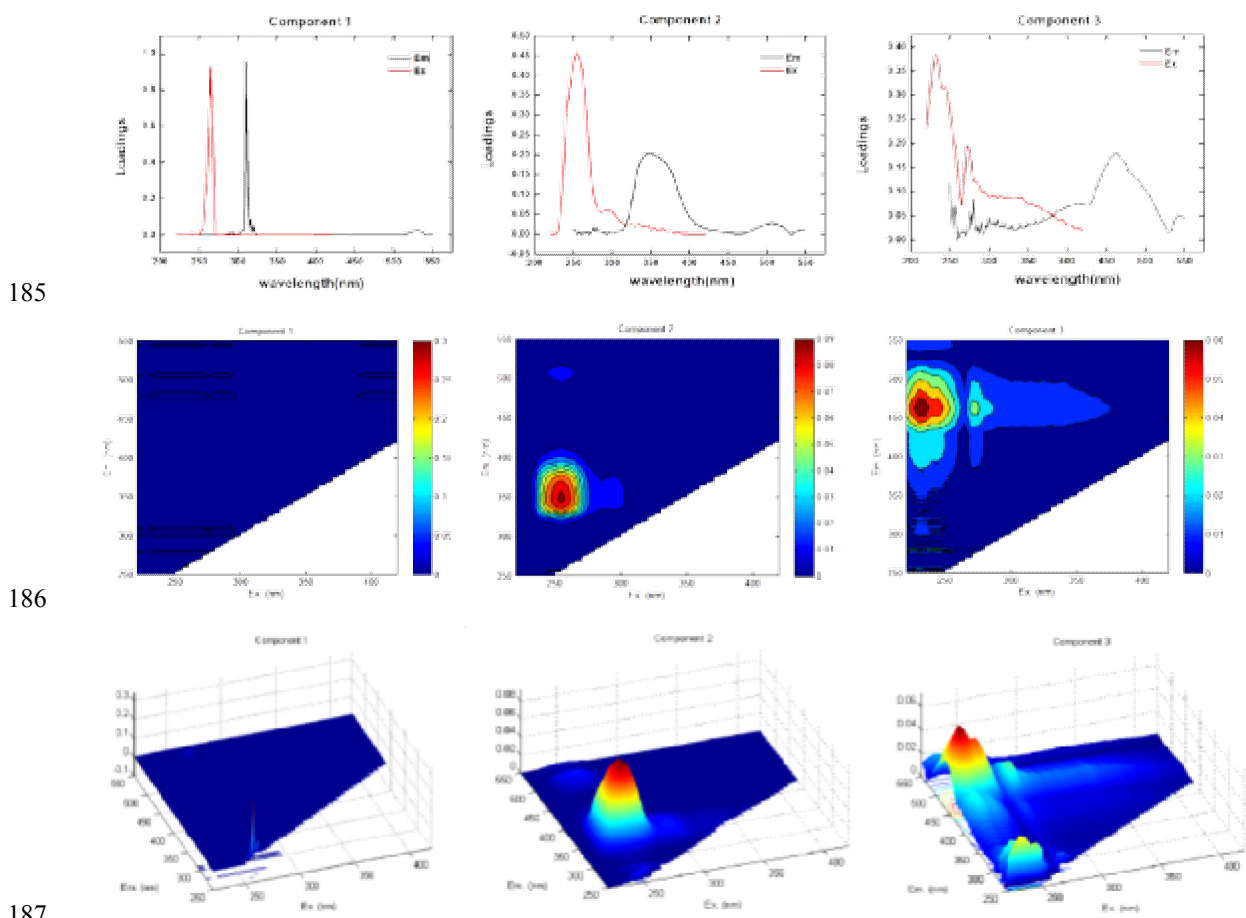
174

The spectral characteristics of three identified components were presented as a function of excitation and emission wavelength, and the fluorescence excitation and emission matrix spectra for three components and corresponding contour plots were shown in Fig 3. As shown in Fig 2, the PARAFAC model identified two protein-like substances (component 1 and component 2) and one humic-like substance (component 3). These components of DOM were confirmed by comparing the excitation/emission characteristic peaks with reported characteristic wavelength of pure substances. For instance, the major peaks of tyrosine and tryptophan were usually detected at Ex/Em=275/310nm and 278/340nm<sup>[46]</sup>, respectively, which were similar to the characteristic peaks of C1(270/310nm) and C2(251/352nm) in our study, thus C1 and C2 were confirmed as tyrosine-like and tryptophan-like substance, separately. Similarly, C3 had Ex/Em characteristics(240, 272/460nm) close to those of fulvic or humic acid whose major peaks were detected at Ex/Em=240-270/430-462nm in freshwater rivers<sup>[47]</sup>. Consequently, C3 was identified as humic-like substance.

C1 had excitation/emission characteristics close to tyrosine(275/310nm)<sup>[46]</sup>, which was related to bacteria degradation of organic material in waters and identified as autochthonous protein-like substances in earlier studies<sup>[29,48,49,50]</sup>. Characterized by peaks of excitation/emission 251nm/352nm, C2 had Ex/Em spectral characteristics similar to that of free amino acids or protein-bound amino acids (component 6) reported by Kowalczyk<sup>[51]</sup>, which assumably represented a fluorescent tryptophan derived from autochthonous DOM. It was observed that the single excitation peak of C2 was blue shifted, while the emission peak was red shifted compared to the spectral characteristics of pure tryptophan, indicating that tryptophan was bound into larger structures of organic molecules instead of pure compounds diluted in the water. According to previous studies, the presence of hydroxyl, alkoxy, amino groups and carboxyl components might accounted for a slight red shift of emission peaks<sup>[52,53]</sup>. Susann<sup>[54]</sup> observed a shift towards smaller molecules in the molecular size distribution of DOM during incorporation to sea ice, with the

175 fluorescence intensity increasing at shorter emission wavelengths, which supposed that a longer  
 176 emission wavelength for C2 might explain the shift towards larger molecules binding to DOM.  
 177 However, additional detailed molecular knowledge is required to characterize DOM in Jiangxi  
 178 region.

179 The fluorescence spectrum of C3 was similar to that of terrestrial humic-like substances  
 180 identified by Yamashita<sup>[55]</sup>. C3 had a primary and secondary excitation peak at 240nm and 272nm,  
 181 respectively, and a single emission peak around 460nm, which were similar to those peaks of  
 182 humic-like PARAFAC components in previous studies<sup>[29,55,56,57]</sup>. These fluorophores have also  
 183 been found in the EEM spectra exhibited by Zeri<sup>[50]</sup>, which suggested the presence of humic-like  
 184 component in coastal environments.



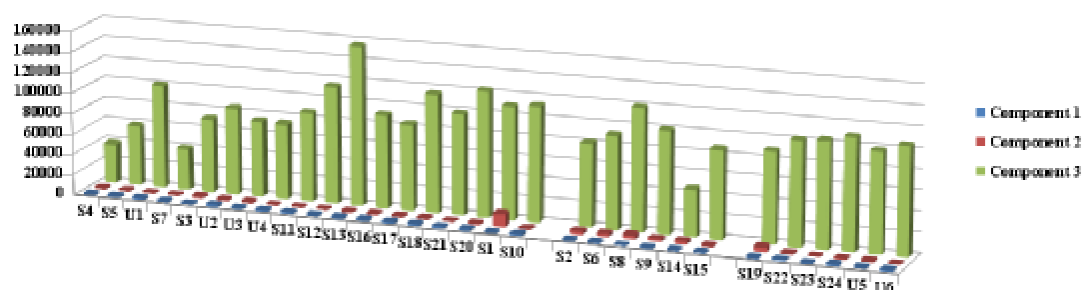
185  
 186  
 187  
**Fig 3. Excitation and emission loadings for the three different fluorescent components, and contour plots identified by PARAFAC model. Intensity is shown as Fmax in Raman Units( $\text{nm}^{-1}$ )**

188

### 189 3.2 Distribution of DOM components in Longnan Ore District.

190 PARAFAC analysis provided quantitative information of DOM fluorescence composition  
 191 concerning the distribution of three components for 30 samples collected at different stations. The  
 192 humic-like substance represented by C3 accounted for the vast majority proportion in the  
 193 composition of DOMs. As illustrated in Fig 4, C3 in S3 and S5, which were located in the west of  
 194 sampling area, constituting 98.3% and 97.6% of the total compound for each sample, respectively,  
 195 and C3 in S2 and S14 acquired from the eastern area took up 96.6% and 94.4%, with protein-like  
 196 substance(component 2) occupying approximately 3% and 5% for each sample. The

197 tryptophan-like compounds(C2) of S1 substantially exceeded tryptophan content of other samples,  
 198 which was probably input from the bank of downstream locations. Similarly, the protein-like  
 199 substance tyrosine (component 1) accounted for merely a tiny fraction(<1%) in DOMs for all the  
 200 samples, indicating that it was typically generated by biological processes in the stream or the  
 201 surrounding environment. Based on the particular basin terrain of Jiangxi Ore district, the DOMs  
 202 of surface or underground water in the middle such as S8, S9, S11, S12, S13, S22, S23, S24, U6  
 203 and U1, were basically higher than those surrounding the center(S2, S4, S5, S7, S15), indicating a  
 204 higher content of protein-like and humic-like substances. However, downstream S18 and S20,  
 205 located in the southwest of the ore district, were considered to be an exception which had higher  
 206 DOMs values, revealing that sources of downstream could be traced back to upstream waters thus  
 207 the downstream waters exhibited fairly high DOM content. S11 and S12 located in the tributary  
 208 shared almost the same DOM value with underground water U2 and U3 in the neighboring  
 209 sampling station, indicating a terrestrial source for S11 and S12 instead of an upstream runoff  
 210 input. Whereas, S13 as the downstream of tributary, presented a significantly higher DOM value  
 211 not only than S11 and S12, but also than the underground water U4 in the vicinity, showing a  
 212 consequence of upstream and terrestrial source. S4 and S5 followed the same trend of DOM  
 213 content as S12 and S13, while the remarkably higher DOM value of U1 could explain the source  
 214 of S5 was generally released from upstream rather than terrestrial source. The distribution of  
 215 components showed minor variations of DOM between stations S19, S22, S23, S24, U5 and U6,  
 216 which testified a homologous source of DOMs for samples in the southern area. The surface water  
 217 samples S2 and S15 collected at almost the same longitude had similar fluorescence intensities,  
 218 which were lower than those of S6, S8, S9 taken in the same longitudinal zone due to its relatively  
 219 high elevation as well as the upstream topography.  
 220



221

**Fig 4 Distribution of three PARAFAC-identified components in DOMs at selected sampling stations. Bar plots indicated the fluorescence intensities of three components for each sample collected at different districts.**

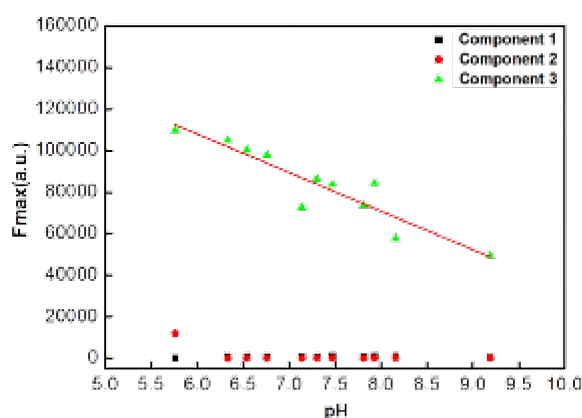
222

### 223 3.3 Behavior of PARAFAC-derived components with changes of pH and concentrations of 224 metals.

225 A negative linear correlation ( $R^2=0.8465$ ) between fluorescent C3 and pH (5.7~9.2) were  
 226 observed in Fig 5, suggesting that fluorescence intensities of humic-like substances were  
 227 influenced by changes in pH, whereas the other two components were basically unrelated to pH  
 228 condition. Dissolved humic substances of DOM was strongly pH-dependence with humic acid  
 229 soluble at  $\text{pH}>2$  and fulvic acid soluble at all pH values, and the fraction of dissolved humics  
 230 would increase with increasing pH<sup>[58]</sup>, in contradict with the results showing a negative relation



231 between pH and fluorescence intensities of humic-like component in our report. Therefore there  
 232 might be other reasons, such as DOM-metal coordination, or the change of molecular weight of  
 233 components caused by pH change, leading to this phenomenon. According to the results reported  
 234 by Pourret<sup>[42]</sup>, the amount of REE bound to humic acid strongly increased with increasing pH,  
 235 indicating that a higher pH stimulates the complexation of REE and humic substances, which  
 236 might reduce the concentration of humic substances with impairing fluorescence intensities. The  
 237 conclusion drawn by Chen<sup>[59]</sup> also confirmed that pH was the key water chemistry parameter to  
 238 regulate DOM binding to metal ions, since the binding affinity to Cu<sup>2+</sup> of Suwannee River fulvic  
 239 acid was remarkably suppressed when lowering pH from 6 to 4, thus consequently causing an  
 240 increase of DOM fluorescence intensity in water samples. In addition, the findings that the  
 241 molecular weights of DOM increased gradually with pH values ranging from 10.5 to 2.5<sup>[60]</sup>, were  
 242 consistent with the results suggesting higher molecular sizes occur with lower pH values<sup>[61]</sup>,  
 243 providing a possible explanation for negative correlation between pH and fluorescence intensity of  
 244 DOM if the molecular weights of DOM fraction were proved to be positively associated with its  
 245 fluorescence intensity. However, the pH values in the middle area of the ore district remained  
 246 stable around 7.0, and the underground water samples (U5, U6) from southern area were slightly  
 247 acidic with pH around 6.5, while the surface water samples nearby(S21-S24) were alkaline with  
 248 pH ranging from 8.3 to 9.5, indicating that the composition of surface water were assumedly  
 249 irrelevant to terrestrial origin.



250

**Fig 5 A linear correlation between fluorescence intensity and pH for three components**

251

252 Recent studies have demonstrated that PARAFAC-EEM quenching could be employed to  
 253 investigate the interactions between metal ions and fluorescent components of DOM from soil and  
 254 water samples<sup>[14,62,63,64]</sup>. Therefore, apart from pH values, the fluorescence quenching effects of  
 255 metals also played a significant role in affecting the fluorescence properties of different  
 256 components identified by the PARAFAC model in EEMs of samples of surface and underground  
 257 waters in the Jiangxi Ore District.

258 As illustrated in Fig 6, a significant quenching of fluorescence intensity of C1 (tyrosine-like  
 259 substances) were observed in the presence of cobalt(Co), nickel(Ni), uranium(U), Th and several  
 260 rare earth elements such as La, Nd, Ce, Pr, Gd, Dy, etc. It was interesting to find that the  
 261 quenching effects of Co and Ni were strong for C1, whereas they were weak for C2, however, the  
 262 presence of copper(Cu) and titanium(Ti) slightly quenched the fluorescence intensity of C2

263 (tryptophan-like material) instead of C1, reflecting that tyrosine-like substances contributed to  
 264 Co/Ni complexation, while Cu/Ti binding was induced by tryptophan-like compound. Obviously,  
 265 strong quenching effects of heavy metals were mostly exhibited in C1 instead of C2 even both of  
 266 them were identified as protein-like components by PARAFAC model, indicating that  
 267 tyrosine-like materials were presumably responsible for metal binding in DOM, thus producing  
 268 non-fluorescent compounds that led to quenching effect, which was consistent with previously  
 269 published results describing the quenching effects of heavy metals on fluorescent protein-like  
 270 components of DOM as a consequence of complexation of metal ions<sup>[14][65]</sup>.

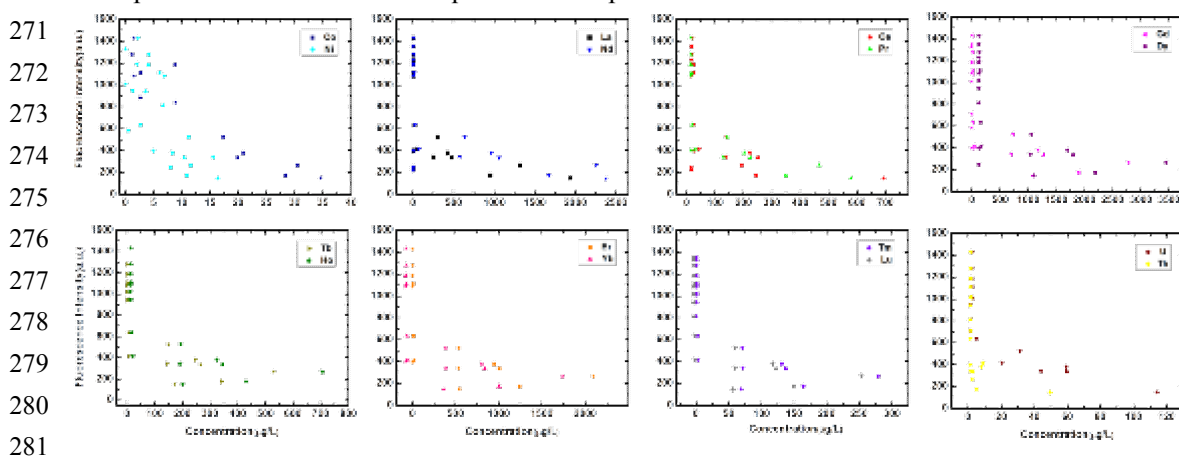


**Fig 6 Changes in the fluorescence intensity of component 1 with the increase of concentrations of Co, Ni and some rare earth metals**

282

283 A positive correlation between C2 and concentrations of various metals were observed with  
 284 the fitting linear equations shown in Fig 7. We could see that concentrations of most of the  
 285 lanthanides, Y and radioactive element U increased linearly with the increase of the fluorescence  
 286 intensity of C2, suggesting that the component of DOM sycophant, due to its high molecular  
 287 weight, hydrophobicity and aromatic functional groups<sup>[32]</sup>, might have a positive impact on the  
 288 adsorption of rare earth metals such as La, Ce, Nd, Sm, Tb, Dy, Ho, Yb, Y, etc, which could be  
 289 used as an indicator to evaluate the capacity of rare earth metal absorption of underground and  
 290 surface water in Jiangxi Longnan Ore District. Previous studies indicated that the dominant  
 291 control on rare earth metal-DOM complexation, was rare earth elements binding to weak sites on  
 292 DOM with relatively high molecular weight in natural terrestrial waters<sup>[66,67]</sup>. Moreover, a  
 293 consistent trend of Tm/Lu and Er/Yb displayed in concentration changes with fluorescence  
 294 intensity, revealing the process of coadsorption of heavy rare earth elements on DOM in surface  
 295 water samples.

296 Yet, despite the fluorescence intensity curves of C3 with concentration changes of U/Th,  
 297 Gd/Dy, Tb/Ho, Tm/Lu and Er/Yb had a similar tendency, there was neither distinct correlation  
 298 observed between fluorescence intensity and metal concentration, nor quenching effect shown in a  
 299 wide range of metal concentrations, thus indicating that humic-like component was likely to  
 300 absorb some metals in a considerably narrow concentration range, but in general irrelevant to the  
 301 formation of new complex coordinated with rare earth elements such as Tm, Yb and Er. In a study  
 302 conducted by Motoki<sup>[68]</sup>, a similar ideas might explain the reason, which proposed that the  
 303 humic-like substances in the DOM of Horonobe groundwater had a lower binding affinity for  
 304 lanthanides and actinides. Whereas, the interaction between dissolved rare earth metals and humic

305 acids was described in some studies<sup>[69,70]</sup>, which discussed the influence of humic acid on the  
306 complexation behavior of lanthanides.

307 Recently, heavy metal pollution of soil, water and sediment has become a hot issue, which  
308 focuses on modes of occurrence, migration of heavy metal pollutants and biotoxicity in the field of  
309 environmental monitoring. DOM can strongly affect metal speciation and the formation of  
310 metal-DOM complexes may alleviate the harm from dissolved metals in soil, water and  
311 sediment<sup>[67][71]</sup>. However, due to the high complexity of components of DOM, not only the  
312 influence of DOM on the behavior of heavy metals in soil, water and sediment remains to be  
313 investigated, but the internal mechanism for the migration and absorption of heavy metals also  
314 requires a further explanation, thus making DOM as an indicator to assess heavy metal chelation  
315 and migration effects.

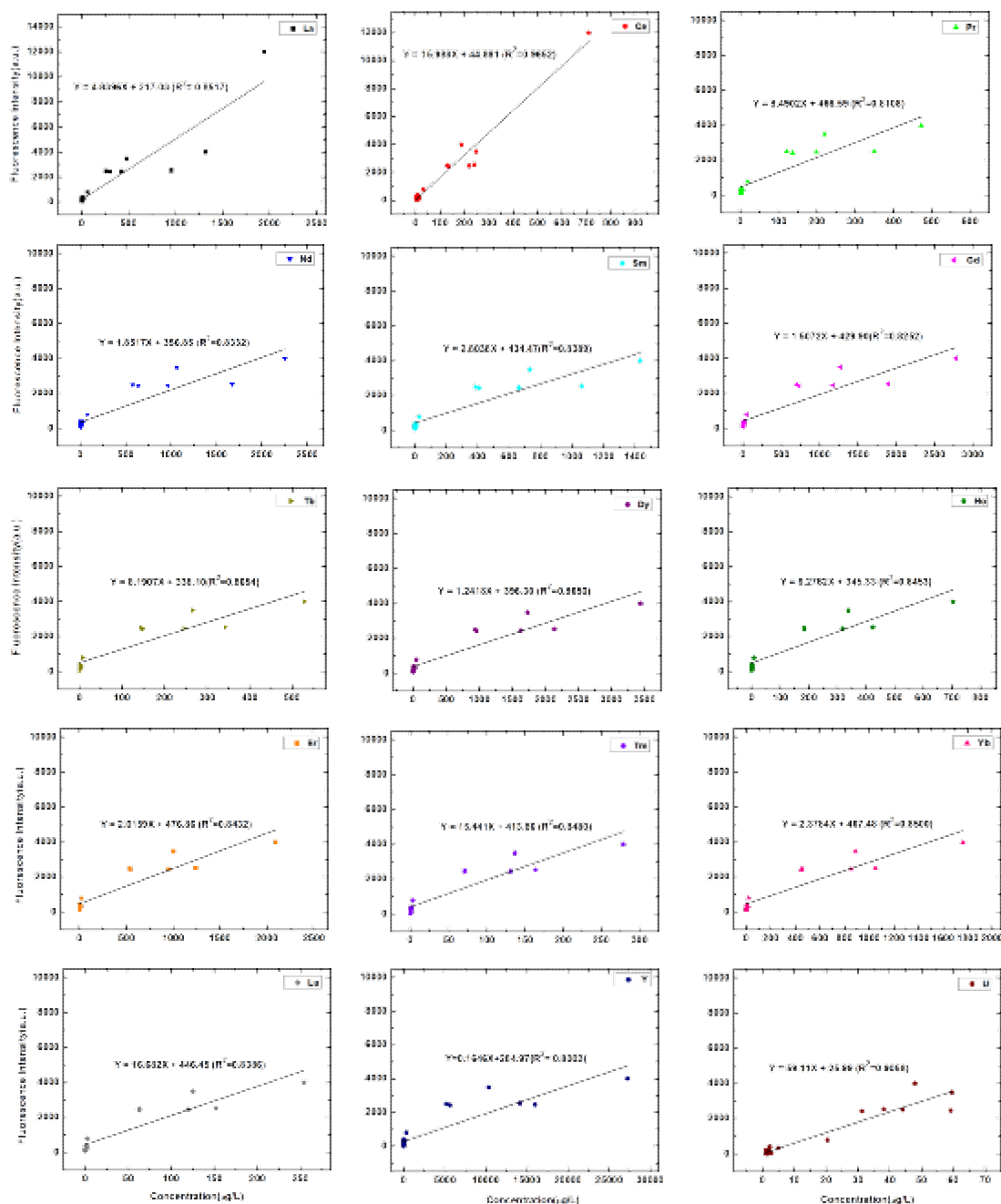


**Fig 7 Relationship between concentration of various rare earth metals and fluorescence intensity of component 2.**

316

## 317 4 Conclusion

318 This study provides information on DOM components of water samples from Jiangxi  
 319 Longnan Ore District with the following conclusions drawn on the basis of EEM-PARAFAC  
 320 analysis: (1) Two protein-like substances(C1 and C2) and one humic-like substance(C3) were  
 321 identified by PARAFAC model. (2) Due to the influence of river flow direction and terrain, the  
 322 fluorescence intensity of DOM components from downstream or in central region was relatively  
 323 higher than that from upstream or surrounding the center. (3) Linear decrease in fluorescence

324 intensity of C3 with the increase of pH was observed, while C1 and C2 was not affected by pH  
325 condition. (4) The quenching effect and linear correlation between protein-like components and  
326 rare earth metals accounted for the metal-DOM complexation and adsorption in water samples.  
327 Results from our study have considerable implications for the role of DOM components on the  
328 toxicity and migration behavior of rare earth metals, and the mechanism of pollutant adsorption  
329 and desorption by organic matter under unique geological settings. Furthermore, it shows  
330 excellent predictions on main chemical structure of organic matter, and critical control factors  
331 based on the capacity and strength of DOM affecting the complexation or adsorption with toxic  
332 metals.

333

### 334 **Acknowledgments**

335 This work was supported by the National Natural Science Foundation of China (Grant No.  
336 41301566 ), China Geological Survey project (Grant No.12120113015400) and International S&T  
337 cooperation program of China (ISTCP) (Grant No.2012DFA21000). We thank two anonymous  
338 reviewers for their helpful comments about the manuscript.

339

### 340 **References**

- 341 1 Campbell J H, Evans R D, *The Science of Total Environment*, 1987, **62**, 219-227.
- 342 2 Wu F, Tanoue E, *Organic Geochemistry*, 2001, **32**, 11-20.
- 343 3 Chiou C T, Malcolm R L, Brinton T I, et al, *Environmental Science Technology*, 1986, **20**,  
344 502-508.
- 345 4 V. Drozdowska, *Oceanologia*, 2007, **49**, 59-69.
- 346 5 E.M. Carstea, A. Baker and R. Savastru, *Water Environ. J.*, 2014, **28**, 11-22.
- 347 6 L. Ghervase, A. Cordier, F. Ibalot and E. Parlanti, *Romanian Rep. Phys.*, 2012, **64**,  
348 754-760.
- 349 7 A. Imai, T. Fukushima, K. Matsushige, Y.H. Kim and K. Choi, *Water Res*, 2002, **36**,  
350 859-870.
- 351 8 M. Filella, J. Buffle and N. Parthasarathy, *Encyclopedia of Analytical Science (Second*  
352 *Edition)*, 2010, 288-298.
- 353 9 E.M. Thurman. *Organic Geochemistry of Natural Waters*. 1985.
- 354 10 G.R. Aiken, *Comprehensive Water Quality and Purification*, 2014, **1**, 205-220.
- 355 11 Ronald Beckett and James Ranville, *Interface Science and Technology*, 2006, **10**, 299-315.
- 356 12 D. Grasso, *Chemosphere*, 1990, **21**, 1181-1197.
- 357 13 Emanuele Organelli, Annick Bricaud, David Antoine and Atsushi Matsuoka,  
358 *Oceanographic Research Papers*, 2014, **91**, 72-85.
- 359 14 Jun Wu, Hua Zhang, Pin-Jing He and Li-Ming Shao, *Water Res.*, 2011, **45**, 1711-1719.
- 360 15 Yamashita and R. Jaffé. *Environ. Sci. Technol.*, 2008, **42**, 7374-7379.

- 361 16 Xin Zhang, Rafael Marcé, Joan Armengol and Romà Tauler, *Chemosphere*, 2014, **111**,  
362 20-128.
- 363 17 Ke Wang, Weiguang Li, XuJin Gong, Yunbei Li, Chuandong Wu and Nanqi Ren,  
364 *International Biodeterioration & Biodegradation*, 2013, **85**, 617-623.
- 365 18 W. Tian, L.Z. Li and F. Liu, *Bioresource Technology*, 2012, **110**, 330–337.
- 366 19 Xiaowei Li, *Bioresource Technology*, 2014, **159**, 412-420.
- 367 20 R.K. Henderson, A. Baker, K.R. Murphy, A. Hambly, R.M. Stuetz and S.J. Khan. *Water*  
368 *Res.*, 2009), **43**, 863–881.
- 369 21 C.A. Stedmon and R. Bro, *Limnol. Oceanogr. Methods*, 2008, **6**, 572–579.
- 370 22 J.B. Fellman, M.P. Miller, R.M. Cory, D.V. D'Amore and D. White, *Environ. Sci. Technol.*,  
371 2009, **43**, 6228–6234.
- 372 23 K.R. Murphy, A. Hambly, S. Singh, R.K. Henderson, A. Baker, R. Stuetz and S.J. Khan,  
373 *Environ. Sci. Technol.*, 2011, **45**, 2909–2916.
- 374 24 Meilian Chen and Rudolf Jaffé, *Water Research*, 2014, **61**, 181-190.
- 375 25 Wilson G. Mendoza and Rod G. Zika, *Progress in Oceanography*, 2014, **120**, 189-204.
- 376 26 Cohen, Guy J. Levy and Mikhail Borisover, *Water Research*, 2014, **55**, 323-334.
- 377 27 Ziegelgruber, KL; Zeng, T; Arnold, WA; Chin, YP, *Limnology and Oceanography*, 2013,  
378 **58**, 1136–1146.
- 379 28 Youhei Yamashita, Rose M. Cory, Jun Nishioka, Kenshi Kuma, Eiichiro Tanoue and  
380 Rudolf Jaffé, *Oceanography*, 2010, **57**, 1478-1485.
- 381 29 Xin Yao et al., *Chemosphere*, 2011, **82**, 145-155.
- 382 30 Youhei Yamashita, Joseph N. Boyer, Rudolf Haffé. *Continental Shelf Research*, 2013, **66**,  
383 136-144.
- 384 31 Fangang Meng, et al., *Water Research*, 2013, **47**, 5027-5039.
- 385 32 Huacheng Xu, et al., *Journal of Hazardous Materials*, 2013, **263**, 412-421.
- 386 33 Yamamoto Y, Takahashi Y, Shimizu H. *Geochem. J.*, 2010, **44**, 39-63.
- 387 34 Jennifer C. Stern, Jeroen E. Sonke, Vincent J.M. Salters. *Chemical Geology*, 2007, **246**,  
388 170–180.
- 389 35 R. Marsac, M. Davranche, G. Gruau and A. Dia, *Geochim. Cosmochim. Acta*, 2010, **74**,  
390 1749–1761.
- 391 36 Olivier Pourret, Me'lanie Davranche, Ge'rad Gruau, Aline Dia. *Geochimica et*  
392 *Cosmochimica Acta*, 2007, **71**, 2718–2735.
- 393 37 J.E. Sonke, *Environ. Sci. Technol.*, 2006, **40**, 7481–7487.
- 394 38 Wei Zhenggui, et al., *Environmental Pollution*, 2001, **114**, 345-355.
- 395 39 Li Jinxia, et al. *Journal of Rare Earths*, 2010, **28**, 957-964.
- 396 40 Martiya Sadeghi, George A. Morris, Emmanuel John M. Carranza, Anna Ladenberger,  
397 Madelen Andersson, *Journal of Geochemical Exploration*, 2013, **133**, 160-175.
- 398 41 Julian Schilling, Clemens Reimann, David Roberts, *Applied Geochemistry*, 2014, **41**,  
399 95-106.

- 400 42 O. Pourret, M. Davranche, G. Gruau and A. Dia, *Chem. Geol.*, 2007, **243**, 128–141.
- 401 43 S.A. Tucker, V.L. Amszi, W.E. Acree, *J. Chem. Educ.*, 1992, **69**, 8–12.
- 402 44 Ohno, T., *Environ. Sci. Technol.*, 2002, **36**, 742–746.
- 403 45 Lakowicz, J.R. *Principles of Fluorescence Spectroscopy*, Third Edition, Springer, 2006.
- 404 46 P. Kowalczyk, W.J. Cooper, R.F. Whitehead, M.J. Durako and W. Sheldon, *Aquat. Sci.*,
- 405 2003, **65**, 384–401.
- 406 47 Khan M. G. Mostofa, Fengchang Wu, et al., *Limnology*, 2010, **11**, 217–231.
- 407 48 C.A. Stedmon and S. Markager. *Limnol. Oceanogr.*, 2005, **50**, 1415–1426.
- 408 49 K.R. Murphy, C.A. Stedmon, T.D. Waite and G.M. Ruiz, *Mar. Chem.*, 2008, **108**, 40–58.
- 409 50 C. Zeri et al., *Journal of Marine Systems*, 2014, **135**, 124–136.
- 410 51 P. Kowalczyk, W.J. Cooper, M.J. Durako, A.E. Kahn, M. Gonsior and H. Young, *Mar.*
- 411 *Chem.*, 2010, **118**, 22–36.
- 412 52 W. Chen, P. Westerhoff, J.A. Leenheer, K. Booksh, *Environ. Sci. Technol.*, 2003, **37**,
- 413 5701–5710.
- 414 53 J. Świetlik, A. Dabrowska, U. Raczyk-Stanislawiak, J. Nawrocki, *Water Res.*, 2004, **38**,
- 415 547–558.
- 416 54 Susann Müller, Anssi V. Vähätalo, Colin A. Stedmon, et al., *Marine*
- 417 *Chemistry*, 2013, **155**, 148–157.
- 418 55 Y. Yamashita, R. Jaffé, N. Maie and E. Tanoue, *Limnol. Oceanogr.*, 2008, **53**, 1900–1908.
- 419 56 Piotr Kowalczyk, *Marine Chemistry*, 2009, **113**, 182–196.
- 420 57 Stephanie K. L. Ishii and Treavor H. Boyer, *Environ. Sci. Technol.*, 2012, **46**, 2006–2017.
- 421 58 Stevenson FJ. *Humus Chemistry: Genesis, Composition, Reactions*, 2nd edn. New York:
- 422 John Wiley & Sons. 1994.
- 423 59 W.B. Chen, D.S. Smith, C. Guéguen, *Chemosphere*, 2013, **92**, 351–359.
- 424 60 M. Safiur Rahman, Marc Whalen, Graham A. Gagnon, *Chemical Engineering*
- 425 *Journal*, 2013, **234**, 149–157.
- 426 61 Vanessa-Nina Roth, Thorsten Dittmar, Reinhard Gaupp, Gerd Gleixner, *Geochim.*
- 427 *Cosmochim. Acta*, 2013, **123**, 93–105.
- 428 62 J. Wu, H. Zhang, P.J. He, L.M. Shao, *Water Res.*, 2010, **45**, 1711–1719.
- 429 63 C. Plaza, G. Brunetti, N. Senesi, A. Polo, *Anal. Bioanal. Chem.*, 2006, **386**, 2133–2140.
- 430 64 J. Zhao, D.J. Nelson, *J. Inorg. Biochem.*, 2005, **99**, 383–396.
- 431 65 Jun Wu, *Journal of Hazardous Materials*, 2012, **215**, 294–301.
- 432 66 Jianwu Tang and Karen H. Johannesson, *Geochimica et Cosmochimica Acta*. 2010, **74**,
- 433 6690–6705.
- 434 67 Jamil A. Sader, Keiko Hattori, Stewart Hamilton and Kerstin Brauneder, *Applied*
- 435 *Geochemistry*, 2011, **26**, 1649–1664.
- 436 68 Terashima M., Nagao S., Iwatsuki T., Fujitake N., Seida Y., Iijima K. and Yoshikawa H.,
- 437 *JOURNAL OF NUCLEAR SCIENCE AND TECHNOLOGY*, 2012, **49**, 804.

- 438 69 Remi Marsac, *Geochimica et Cosmochimica Acta*. 2011, **75**, 5625-5637.
- 439 70 Ralf Kautenburger, et al., *Analytica chimica acta.*, 2014, **816**, 50-59.
- 440 71 Perdue, E.M. and Ritchie, J.D., *Treatise on Geochemistry*, 2005, 273–318.
- 441



442 Figure Captions

443 **Fig 1.** location of the sampling sites

444

445 **Fig 2.** Examples of measured, modeled and residual EEMs for sample collected from sites of  
446 S2(2), S8(9), S14(18), S19(23). Fluorescence is shown in Raman Units ( $\text{R.U.nm}^{-1}$ )

447

448 **Fig3.** Excitation and emission loadings for the three different fluorescent components, and  
449 contour plots identified by PARAFAC model. Intensity is shown as  $F_{\text{max}}$  in Raman Units( $\text{nm}^{-1}$ )

450

451 **Fig 4.** Distribution of three PARAFAC-identified components in DOMs at selected sampling  
452 stations. Bar plots indicated the fluorescence intensities of three components for each sample  
453 collected at different districts

454

455 **Fig 5.** A linear correlation between fluorescence intensity and pH for three component

456

457 **Fig 6.** Changes in the fluorescence intensity of component 1 with the increase of concentrations  
458 of Co, Ni and some rare earth metals

459

460 **Fig 7.** Relationship between concentration of various rare earth metals and fluorescence  
461 intensity of component 2

462

463

